The Intrinsic Nature of Rapid Mineralization of CO_2 in Peridotites-Data Reproduction from a pilot test site

Introduction

Peridotite is an ultramafic igneous rock predominantly composed of olivine and pyroxene, chemically characterized by extremely low SiO_2 (<45%) and exceptionally high Mg and Fe contents (Kelemen et al. 2011). This feature provides a pathway to overcome the instability barrier in geological CO_2 sequestration, enabling rapid and stable mineral trapping.

Global peridotite outcrops demonstrate that natural carbonation rates are already exceptionally high. Studies estimate that the Semail ophiolite (a rock suite containing peridotite) naturally sequesters approximately 10^4 to 10^5 tons of CO_2 annually (Kelemen et al. 2008). Similar peridotite massifs include the Atlin ophiolite in British Columbia, Canada; the Chenaillet ophiolite in France; the Erro-Tobbio massif in Italy; as well as the Luobusa ophiolite in Tibet and the Dalabute ophiolite in Xinjiang, China (Hansen 2005, Bonnemains et al. 2016, Valentin et al. 2019, Qiu et al. 2018). If geological CO_2 sequestration in peridotite can be fully realized, the goal of global net-zero CO_2 emissions will be within reach.

Current research on peridotite carbon sequestration involves field outcrop investigations, laboratory experiments, and field tests (Qiu et al. 2018, Snaebjörnsdóttir et al. 2020). While outcrop investigations reveal the natural carbonation processes of atmospheric CO_2, laboratory experiments primarily focus on underlying reaction mechanisms. Although field tests offer insights into in-situ CO_2 mineralization, relying solely on aqueous data is insufficient to reconstruct subsurface reaction dynamics.

Therefore, based on the rapid CO_2 mineralization field test data from shallow peridotites in Oman (Matter et al. 2025), this study successfully constructed a geochemical reaction model to simulate the test process. This approach reveals and quantifies the complex, invisible geochemical reactions within the formation, providing theoretical support and potential prediction for CO_2 storage in peridotite reservoirs.

Initial Parameter Inversion and Model Validation

Geochemical simulations were conducted using the TOUGHREACT simulator based on a single well push-pull field tests in peridotite formations. The simulation included a 0.6-day CO_2-saturated water injection, a subsequent 45-day storage, and an 11.2-day pumping.

To constrain the unknown key physical properties of initial porosity and permeability, their ranges were first estimated from well-test data. Subsequently, parameter inversion was performed using the Bayesian-optimized Tree-structured Parzen Estimator (TPE) algorithm, with the concentration of the conservative tracer Br^- during the pumping phase as the objective function.

The same inversion approach was applied to determine the initial compositions of four primary minerals: forsterite, chrysotile, enstatite, and chalcedony. However, the objective functions for this mineralogical inversion were the concentration variations of DIC (Dissolved Inorganic Carbon—the sum of HCO_3^-, CO_3^{2-}, and $CO_2(aq)$), Ca^{2+}, Mg^{2+}, and $SiO_2(aq)$) during the pumping period. Unlike the Br^- tracer, the concentrations of these species are governed by the interplay of physical transport and geochemical reactions.

These two inversions were executed sequentially to reconstruct the initial formation conditions by fitting simulation results to field data, successfully modeling the multi-stage field test.

Migration and Evolution Characteristics of CO_2-Saturated Water

The variations in ion concentrations at the injection point reflect the temporal evolution characteristics of the CO_2-saturated water at a specific location within the formation (blue curve in Fig. 1). To accurately quantify the contribution of geochemical reactions, this study introduced and developed an End-member Mixing Model. By utilizing the concentration profile of the conservative tracer Br^- as a baseline, the concentration changes induced by physical diffusion were decoupled, thereby deriving the net geochemical contribution (ΔC_{geo}) for each ion species (orange curve in Fig. 1). A value of $\Delta C_{geo}>0$ indicates mineral dissolution releasing ions into the aqueous solution, whereas $\Delta C_{geo}<0$ signifies mineral precipitation consuming ions from the solution.

The elevation in pH is almost exclusively driven by geochemical reactions; although this contribution decreases slightly towards the end of the storage period, it still accounts for 84.4%. In contrast, the variation in DIC is almost entirely governed by physical diffusion during the early storage phase, with the geochemical contribution reaching only 16% by the end of storage.

This contrast highlights the asynchrony between silicate mineral dissolution and carbonate mineral precipitation. This behavior is fundamentally controlled by pH: in acidic environments with lower pH, silicate dissolution dominates while carbonate precipitation is inhibited. As pH continues to rise, geochemical reactions become dominated by carbonate precipitation. The rapid decline in Ca^{2+} and Mg^{2+} concentrations after 20 days corresponded to the rapid carbonate precipitation phase, occurring at a pH of 6.4. Furthermore, the variation in SiO_2(aq) concentration is dictated by geochemical reactions, reflecting the balance between silicate dissolution and chalcedony precipitation.

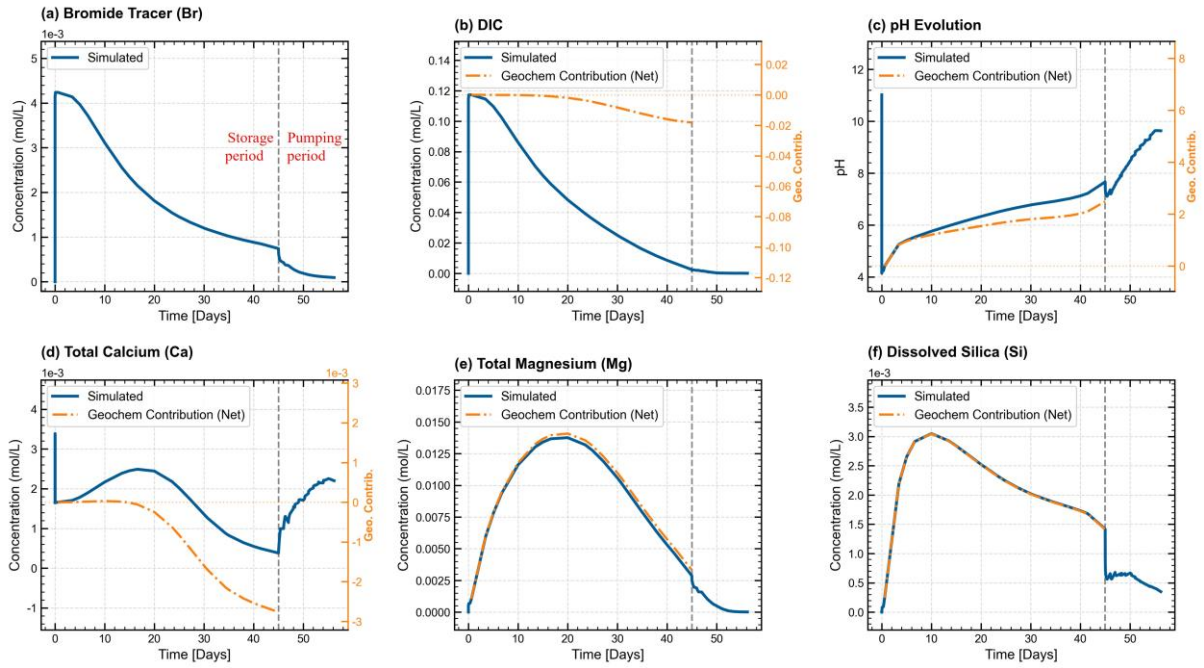

Figure 1 *Variations in ion concentrations at the injection point and the net geochemical contribution (ΔC_{geo}).*

Spatiotemporal Evolution Characteristics of Geochemical Reactions

All spatial distribution maps for ions and minerals are presented as X-Z cross-sections with the well located at the left boundary. The abundant Mg^{2+} released from the initial mineral dissolution, coupled with the elevated Ca^{2+} concentration in the formation water, synergistically drive the precipitation of carbonate minerals. Figure 2(a) illustrates the concurrent processes for Mg^{2+}: its consumption via mineral carbonation at the injection front and its continuous supply from mineral dissolution behind the front.

Figure 2(b) demonstrates that during the early storage period (prior to 20 days), the behavior of Ca^{2+} is dominated by fluid mixing. A concentration gradient induced by molecular diffusion is clearly visible near the wellbore, while a precipitation band of Ca-bearing carbonates forms at the front. As time evolves, intense carbonation takes place within the reaction zone, whereas the front boundary region is governed by the dual effects of continuous molecular diffusion and mineralization.

The migration and spatial distribution of ions elucidate the spatiotemporal evolution patterns of carbonate mineral precipitation (Figure 2 (d), (e) and (f)). Calcite, being the most readily precipitated carbonate, begins to form during the injection phase. At the advancing front—characterized by high pH (>7) and a low Mg^{2+}/Ca^{2+} ratio (where Mg^{2+} remains near its original formation concentration)—calcite precipitates initially. This is subsequently replaced by dolomite (dolomitization) and is ultimately dominated by magnesite.

This dynamic mineralogical evolution at the injection front is driven by the continuous diffusion of acidic fluids and the massive release of Mg^{2+} from silicate dissolution, which jointly lower the pH and elevate the Mg^{2+}/Ca^{2+} ratio. Fostered by its favorable moderately-to-weakly alkaline conditions and high Ca^{2+} concentration, the injection front acts as the active "frontline" for CO_2 mineralization, following a precipitation sequence of: calcite > dolomite > magnesite.

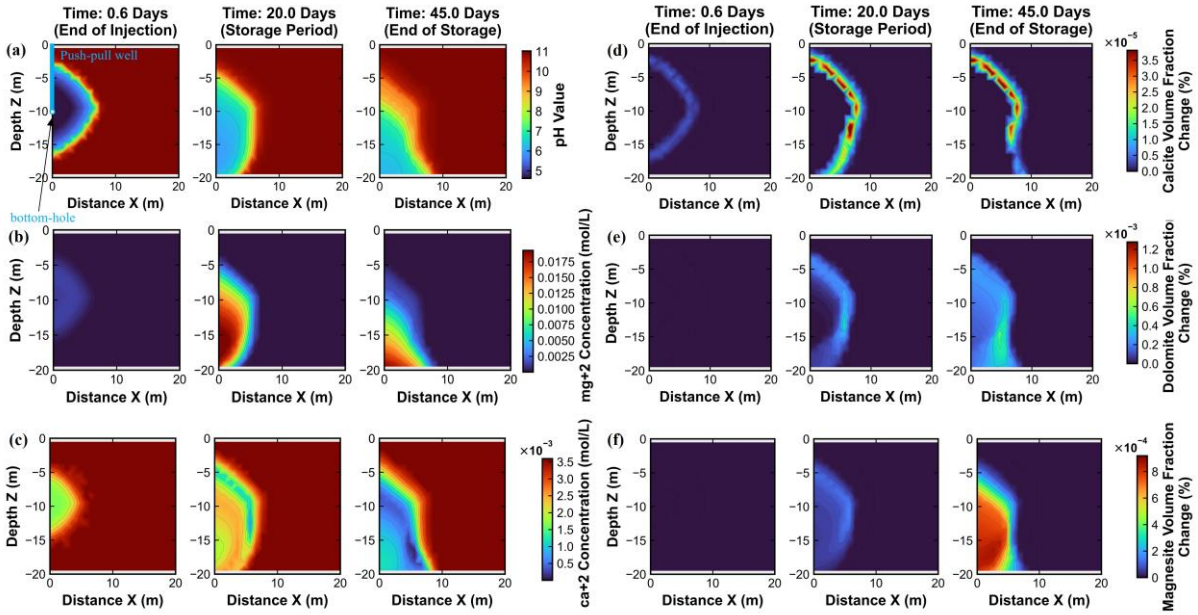

Figure 2 *Spatiotemporal evolution of geochemical reactions within the formation during the storage period: (a) pH value; (b) the concentration of Mg^{2+}; (c) the concentration of Ca^{2+}; (d) the volume fraction change of calcite; (e) the volume fraction change of dolomite; (f) the volume fraction change of magnesite.*

Conclusions

An asynchrony exists between the initial dissolution of silicate minerals and the precipitation of carbonate minerals. In the acidic environment following the injection of CO_2-saturated water, silicate minerals dissolution dominates, releasing abundant Mg^{2+}, whereas carbonate precipitation is inhibited. As the pH rises above 6, silicate dissolution decelerates, and carbonate precipitation becomes the dominant geochemical reaction.

The precipitation of carbonate minerals is strictly controlled by pH and the Mg^{2+}/Ca^{2+} ratio. During the dynamic advancement of the injection front, the precipitation sequence follows the order of calcite >

dolomite > magnesite. Notably, the carbon sequestration contribution of these three minerals is inversely proportional to this sequence.

Over the 45-day storage period, 48.6% of the CO_2 is converted into stable mineral phases via geochemical reactions. Extending the storage duration tenfold increases the mineral trapping ratio to 94.3%, demonstrating the immense potential for rapid CO_2 mineralization within peridotite formations.

Acknowledgements

This work has been supported by the National Key Research and Development Program of China under Grant (No. 2024YFE0213100), the National Foreign Expert Program (No. H20250361) and the Hainan Provincial Natural Science Foundation of China (No. 426MS0384).

References

Bonnemains, D., Carlut, J., Escartín, J., Mével, C., Andreani, M., and Debret, B. [2016]. Magnetic signatures of serpentinization at ophiolite complexes. *Geochem. Geophys. Geosyst.*, **17**, 2969–2986.

Hansen, L. D. [2005]. Geological setting of listwanite, Atlin, BC: implica-tions for carbon diozide sequestration and lode-gold mineraliza-tion. *Vancouver: University of British Columbia*.

Kelemen, P. B., Matter, J. M. [2008]. In situ carbonation of peridotite for CO_2 storage. *Proc Natl Acad Sci USA*, **105**(45): 1729517300.

Kelemen, P. B., Matter, J. M., Streit, E. E., et al. [2011]. Rates and mechanisms of mineral carbonation in peridotite: Natural processes and recipes for enhanced, in situ CO_2 capture and storage. *Annual Review of Earth and Planetary Sciences*, **39**, 545 -576.

Matter, J. M., Speer, J., Day, C. et al. [2025]. Rapid mineralisation of carbon dioxide in peridotites. *Communications Earth & Environment,* **6**, 590.

Qiu, T., and Zhu, Y. F. [2018]. Chromian spinels in highly altered ultramafic rocks from the Sartohay ophiolitic melange, Xinjiang, NW China. *Journal of Asian Earth Sciences* ,**159**, 155 -184.

Qiu, T., Zhu, Y. F. [2018]. Listwaenite in the Sartohay ophiolitic mélange (Xinjiang, China): A genetic model based on petrology, U-Pbchronology and trace element geochemistry. *Lithos*, **302-303**, 427-446.

Snaebjörnsdóttir, S. Ó., Sigfússon, B., Marieni, C., et al. [2020]. Carbon dioxide storage through mineral carbonation. *Nature Reviews Earth & Environment*, **1**, 90-102.

Valentin, B., Elisabetta, R., Laura, C., Carlotta, F., Benoit, I., Marguerite G. [2019]. Multi-stage Reactive Formation of Troctolites in Slow-spreading Oceanic Lithosphere (Erro–Tobbio, Italy): a Combined Field and Petrochemical Study, *Journal of Petrology*, **60**(5), 873–906.